Synthesis and Fundamental Structural Analysis of Composite PVC Latices

SHINZO OMI,* EISUKE SHIIYAMA, KAZUYOSHI AITA, MASATOSHI MATSUMOTO, and MAMORU ISO, *Department of Chemical Engineering, Tokyo University of Agriculture and Technology, Koganei, Tokyo 184,* and MITSURO SAKAYA, AKIRA NAKANO, and YASUTA IMAZAWA, *Research and Development Center, Japan Zeon Co. Ltd., Kawasaki 210, Japan*

Synopsis

Syntheses of various combinations of composite particles were carried out employing PVC-based latices, PVC, PVC–VAc and PVC–VD, as seed particles. Monomers for seed polymerization were chosen so that the solubility in water and the compatibility with seed polymer may influence the features of products. MMA, whose coverage improves the flow characteristics of PVC plastisols to a great extent, was most investigated along with MMA-ST, BMA, and ST. Smaller monomer–polymer feed ratio (M/P), smaller seed size, and the employment of monomers sparsely soluble in water were the key factors in preventing the nucleation of secondary particles during the seed polymerization. A quantitative correlation to evaluate how effectively monomer is converted for the formation of composite particles was proposed. Analyses by means of the electron microscopy (TEM and SEM), GPC, DSC, and TLC strongly anticipated the development of IPN structure and the formation of graft linkage between PVC–VAc core and PMMA.

INTRODUCTION

Modification of polyvinyl chloride (PVC) latices have been extensively investigated to improve dynamic behaviors of plastisols in which PVC particles compose the dispersed phase.[1] Incorporation of monomers such as vinyl acetate (VAc) and vinyliden chloride (VD) to copolymer chains is one of the promising techniques to modify the properties of plastisol. Meanwhile recent development in the synthesis of composite latex particles has added a new dimension to the modification of plastisol.

Oikawa[2] has recently proposed that the dynamic behavior of PVC plastisol was remarkably improved adopting the composite structure with an original PVC latice covered with polymethyl methacrylate (PMMA) shell. The improved properties can be demonstrated as follows. Flow characteristics of the plastisol were improved. For example, PVC–VAc latices covered with PMMA shell behaved as a pseudoplastic fluid when mixed with dioctyl phthalate (DOP), while the original sol remained Newtonian. Latices of larger particle size were acceptable as a base dispersant. Storage period increased without losing the favored flow characteristics.

These encouraging improvements prompted the present authors to investigate more fundamental features to understand the particular properties of

* To whom correspondence should be addressed.

Journal of Applied Polymer Science, Vol. 41, 631–646 (1990)
 CCC 0021-8995/90/3-40631-16$04.00

the plastisol that may lead to other possible combinations of composite systems. The investigation and objectives of this study are summarized as follows.

1. To obtain composite latices employing the following combinations of core latices and monomers, the latter being presumed to compose the shell structure.
   a. Core latex: PVC, PVC–VAc, and PVC–VD. PMMA and PS were briefly employed to obtain additional information.
   b. Shell monomer: MMA, MMA–styrene (ST), and ST. *N*-Butyl methacrylate (BMA) was employed as a polar but less water-soluble monomer (0.08 wt % against 1.7 wt % for MMA[3]).
2. To propose a simple correlation to evaluate the yield of shell monomer incorporated to the composite particles other than wasted to the nucleation of secondary particles.
3. To find out the operational conditions effective to suppress the nucleation of secondary particles (new crop).
4. To estimate the structural features from the information provided from instrumental analyses such as SEM, TEM, GPC, TLC, and DSC.

Direct observation of structured morphology has been provided by means of TEM employing the staining technique. Vanderhoff[4] demonstrated the sophisticated procedure including background (negative) staining as well as conventional positive staining. Newly explored reagents for staining, phosphotungstenic acid for the former and RuO_4 for the latter procedure, have dramatically showed the domains between polyacrylates, PS, and related copolymers, all of these having been regarded as undetectable with OsO_4. Though being not so straightforward as the work of Vanderhoff, substantial information of composite structure can be obtained from the analyses employed by the authors.

Among those core latices, PVC–VAc was most extensively studied, since the suppression of the formation of secondary particles was difficult, in particular, with the combination of MMA shell monomer, which is fairly soluble in the aqueous phase.

All the experimental works were performed batchwise; results of stage-feed and semicontinuous operations will appear in a future article.

EXPERIMENTAL

Materials

Seed (Core) Latices. Employed core latices acting as seed polymer particles are listed in Table I together with the fundamental properties. PVC, PVC–VAc, and PVC–VD were synthesized by Japan Zeon Co. Ltd. using a commercial production facility, while PMMA and PS were prepared with an ordinary batch operation under the surfactant-free recipe.

Shell Monomers. MMA, ST, and BMA were all commercial grade and distilled under vacuum to remove inhibitors. They were stored in a refrigerator prior to use.

TABLE I
Properties of Seed Polymer Particles

Polymer	Wt % of VCM[a]	Average diameter (nm)	Mol wt ($\times 10^{-4}$)		Coverage area of soap[b] (A^2/molecule)
			M_w	M_n	
PVC	100	230	11.0	6.0	40
PVC–VAc	83.6	505	13.0	6.7	50
PVC–VD	70.2	380	9.1	3.4	79
PMMA	—	562	70.8	18.8	99
PS	—	862	38.8	5.1	53

[a] VCM = vinyl chloride.
[b] Sodium lauryl sulfate.

Other Chemicals. Sodium lauryl sulfate (SLS) was the grade for biochemical use and tenside analysis (Merck) and was used without further purification. Ammonium persulfate (Kanto Chemicals Co. Ltd.) was reagent grade and used as an initiator as served.

Seed Polymerization

A five-neck, 1-L separable glass flask was employed as a stirred vessel reactor, equipped with a semicircular Teflon blade. On the top, the flask is equipped with a nitrogen inlet and outlet, an opening to insert a thermocouple, and an inlet for initiator solution. The nitrogen outlet was connected to a condenser to trap condensates. The bottom of the flask has a sampling device and an auxiliary nitrogen inlet. The latter is used to purge dissolved air in the reactant mixture as well as to return excess amount of the mixture to the reactor after a sample was withdrawn.

Standard recipe for the polymerization is shown in Table II. The M/P row in the table indicates the feed weight ratio between shell monomer and core polymer.

TABLE II
Standard Recipe of Seed Polymerization

Seed polymer (g solid)	11.3, 22.5, 45
Monomer (g)	22.5, 45, 90
M/P	0.5, 1.0, 2.0, 4.0, 8.0
Water (g)	415–515
Sodium lauryl sulfate (g)	0.20[a]
APS[b] (g)	0.28
Total (g)	550
Reaction temperature (°C)	60
Agitation rate (min^{-1})	350

[a] 0.3 g of soap was added to stabilize the latex after an extensive heat generation.
[b] Ammonium persulfate.

Seed latex of known solid content was stirred with the carefully weighed monomer for 15–30 min at room temperature. The mixture was then charged in the reactor, and the temperature was raised to a desired level, while a continuous flow of nitrogen is supplied from the bottom. After 30 min elapsed from the onset of nitrogen flow, and the temperature being under control, an initiator solution also bubbled with nitrogen was introduced. The reaction was then carried out under the nitrogen atmosphere.

As a pretreatment to prevent the formation of secondary particles during the seed polymerization, the latex was dialyzed under the continuous flow of tap water at least for one week to remove as much of the adsorbed soap molecules. Only a small amount of SLS, far below the CMC, was added to the reactant mixture. On the contrary, to maintain the shelf stability of latex product, 20 mL of the soap solution containing 0.3 g of SLS was added to the mixture after an extensive heat generation was observed at the later stage of the reaction.

Treatment of Latex Samples

Samples withdrawn were poured into methanol that contained enough hydroquinon to kill the active species, and then precipitated polymers were separated by centrifuge, dried overnight in an oven, and weighed to calculate the yield. This polymer served as the sample for GPC and TLC analysis.

Separation of Composite Particles

For the latex products in which composite and secondary particles were observed, separation of the former was carried out as shown in Figure 1. The latex sample was diluted with the aqueous solution of hydroquinon in a centrifuge cell, and centrifuged for 20 min under 4000*g*. After the decantation, it was confirmed from SEM photographs that the precipitate contained only larger (seed grown) particles. The precipitate was dried under vacuum to retain the original structure, and served as a sample for DSC measurement, and also for electron microscopy.

Analyses of Latex Particles and Polymers

General features of polymer particles were observed with SEM (JEOL, JSM-35CFII), and the average diameter was calculated by measuring the diameter of particles in the photographs. TEM (JEOL, H-3000) was also employed whenever the structure analysis was required.

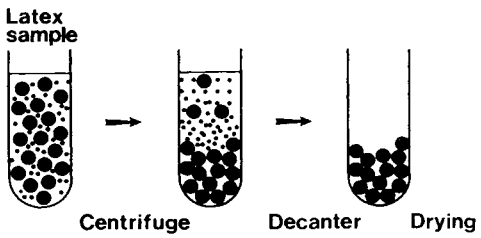

Fig. 1. Separation of composite particles from secondary particles.

Coverage area by a single SLS molecule was measured by the soap titration technique.

Average molecular weight and molecular weight distribution were measured with GPC (HLC-801, Toso Co. Ltd.) employing tetrahydrofuran (THF) as a solvent. Polymer sample was dissolved in THF, and gel fraction was filtered prior to injection.

DSC measurement of polymer samples was carried out employing DT-30 (Shimadzu Co. Ltd.), the rate of heating being fixed at 20°C/min for the measurement of demixing temperature, and 15°C/min for those of the transition temperatures.

When the latter measurement was conducted, the first run was interrupted at around 130°C to exclude impurities such as unreacted, volatile monomers and so on, the presence of these being detected as the inconsistent noises in the curve. The second and the third measurements after inserting enough cooling period, normally 15 min in the atmosphere, yielded reproducible data. The data processed from the second and the third measurements were used for the discussions.

TLC measurement was carried out by means of Iatroscan TH-10 TLC/FID Analyzer (Iatron Lab. Inc.) with various solvents and mixtures. A particular procedure to develop and separate high molecular weight polymers was proposed. Instead of using a conventional cell for the development, a test tube with a tight stopper was used for each chromarod, a porous ceramic rod coated with adsorbents. After the sample solution was spotted, the chromarod was placed in the test tube filled with a small portion of developing solvent. When the level of rising solution reached the half length of the rod, the development was interrupted, and the rod was removed and put in a drying oven to allow the solvent to evaporate. The second development was also interrupted when the rising level reached to three-quarters of the rod, and the rod was dried as already described. Finally in the third development, the rising level was allowed to reach to the full height of the rod. After final drying, the rod was served for FID analyzer.

RESULTS AND DISCUSSION

General Feature of Seed Polymerization

Typical elapsed time curves of the polymer yield are shown in Figure 2 with PVC–VAc seed latex, and M/P being fixed as 2.0. The rate of polymerization of MMA (No. 21) was much higher than that of ST (No. 19). The comonomer run (No. 24) revealed an intermediate feature between the two—almost the same reaction rate in the initial stage as No. 19 and an enhanced gel effect in the later stage as observed in No. 21. The slight decrease of polymer yield observed at the last stage of reaction was due to the dilution of the mixture by an addition of SLS solution. The formation of secondary particles was observed in each run.

The results of molecular weight measurement are listed in Table III. Naturally the distribution of shell polymer overlapped with that of core polymer, and the resultant distribution became broader. Enhanced gel effect and probable formation of the graft linkage between core and shell may have brought the

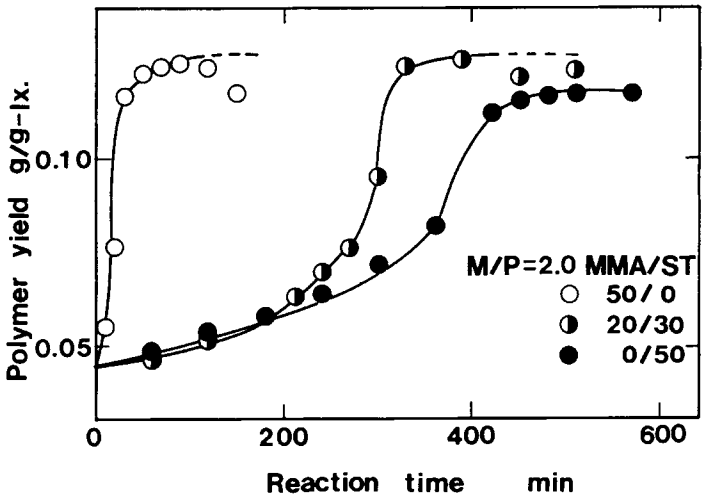

Fig. 2. Profile of polymer yield with elapsed reaction time; PVC–VAc seed.

higher overall molecular weight of PVC–VAc/PMMA than that of PVC–VAc/PS. This possibility will be investigated later.

Structural Analysis of Composite Particles

SEM photographs of composite particles are shown in Figure 3, PVC–VAc/PMMA in (a) and (b), and PVC–VAc/PS in (c) and (d), respectively, with two magnifications. With lower magnification employed [Fig. 3(a) and (c), × 10,000], the difference in the shape of particles is barely noticeable, whereas PVC–VAc/PS particles [Fig. 3(d), × 30,000] are clearly nonspherical compared with those of PVC–VAc/PMMA [Fig. 3(b)], which remain spherical. A further evidence was obtained from the TEM photograph shown in Figure 4(a). Since styrene is incompatible with PVC–VAc copolymer, the structured shell of PS developed on the seed particle as sketched in Figure 4(b).

On the other hand, because PMMA is compatible with PVC–VAc,[5,6] the considerable swelling period prior to the initiation may have enhanced the development of the IPN structure. With this concept TEM photographs of PVC–VAc/PMMA particles stained with RuO_4 were taken and are shown in Figure 5(a). Though it may not be clear in Figure 5(a), original photographs unquestionably reveal the shrinking dark core surrounded with the background

TABLE III
Molecular Weights of Polymers Obtained from the Experiments Shown in Fig. 2

Polymer	M_w (× 10^{-4})	M_n (× 10^{-4})	M_w/M_n
PVC–VAc	15.2	6.2	2.5
No. 21 MMA/ST (50/0)	108	9.8	11.3
No. 24 MMA/ST (20/30)	57.9	6.5	8.9
No. 19 MMA/ST (0/50)	70.2	9.3	7.6

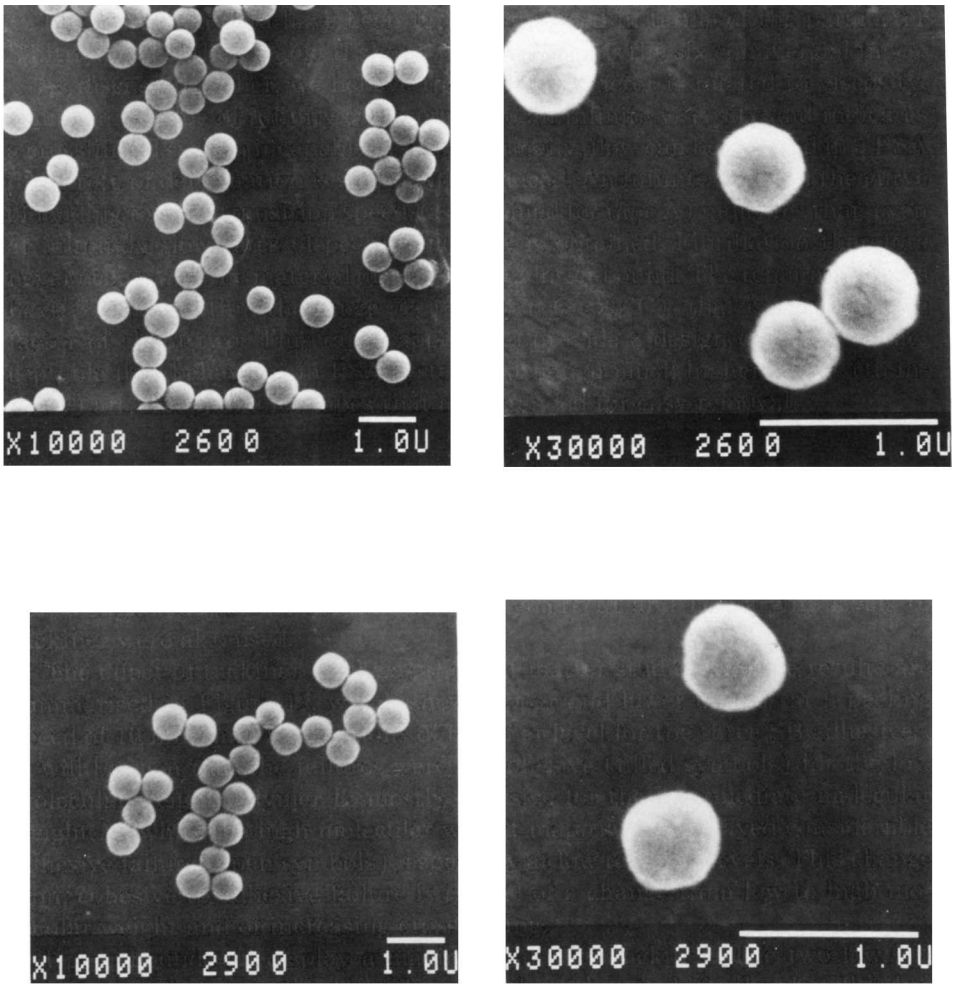

Fig. 3. SEM photographs of composite polymer particles; PVC–VAc seed, $M/P = 1.0$. (a) #26 PVC–VAc/PMMA (× 10,000); (b) #26 PVC–VAc/PMMA (× 30,000); (c) #29 PVC–VAc/PS (× 10,000); (d) #29 PVC–VAc/PS (× 30,000).

shadow that is fading out toward the edge. Almost transparent, there is an outermost shell.

Because PVC–VAc is easily stained with RuO_4, the dark core, off-centered occasionally, can be identified as the remnant of PVC–VAc core unswollen or sparsely swollen with MMA. The shadowy shell reveals the structured domain due to the polymerization of swollen MMA, whose gradient corresponds to the fading shadow toward the edge. The outermost, thin PMMA shell is formed in the final stage of the reaction, in a majority of cases due to the polymerization of MMA dissolved in the aqueous phase.

The preceding discussion leads one to draw the model of the morphology of PVC–VAc/PMMA particles as shown in Figure 5(b). The size of the remaining core of PVC–VAc will depend on the preswelling period and may completely disappear if the equilibrium of swelling is attained. A michrotomed specimen

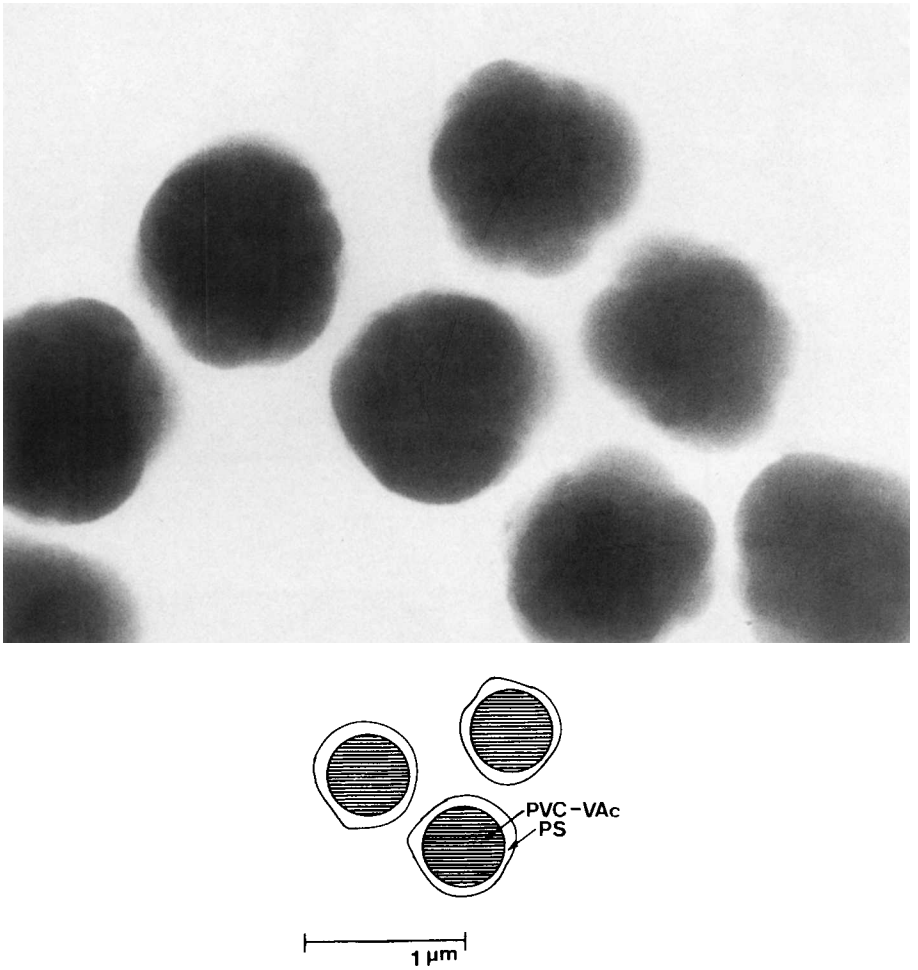

Fig. 4. TEM photograph of PVC–VAc/PS and sketch of morphology. (a) TEM photograph, #29; (b) sketch of particle morphology.

of the dried particles, embedded in epoxy resin and stained with RuO_4, was also observed with TEM; however, no further information has been obtained.

As far as the observations with SEM are concerned, seed polymerizations of PVC-based seeds (PVC–VAc, PVC, and PVC–VD) employing acrylic monomers (MMA and BMA) retained the original sphere, whereas nonspherical particles were intermixed with the spherical ones in the case of PVC–VAc seed with MMA–ST 20 : 30 comonomer. Further study of electron microscopy is being done related to the semicontinuous, starved monomer feed operation.

Fraction of Monomer Spent for the Growth of Seed Polymer Particles

During the synthesis of composite latex, monomer may not be necessarily consumed for the growth of seeds. In the laboratory synthesis, whatever so-

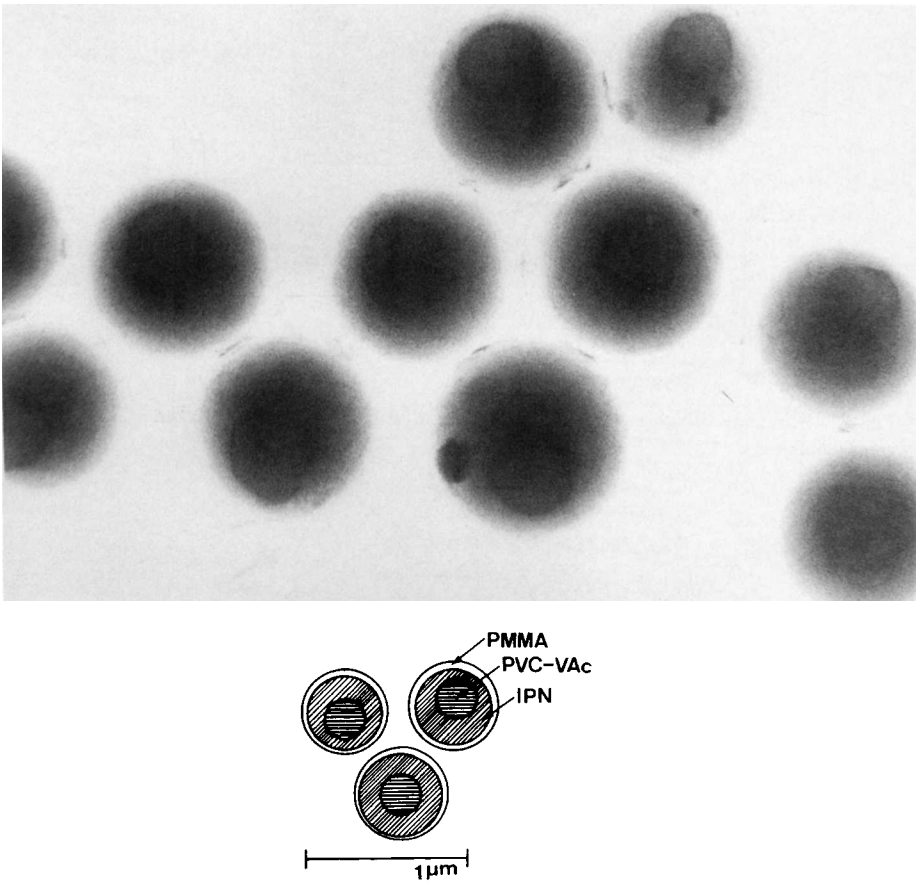

Fig. 5. TEM photograph of PVC–VAc/PMMA stained with RuO_4 and sketch of morphology proposed. (a) TEM photograph, #26 stained with RuO_4; (b) sketch of particle morphology proposed.

phisticated analysis is possible to detect the formation of secondary particles, the circumstance around the commercial process may not allow such a time-consuming analysis. Instead a straightforward correlation will be more desirable, if it gives a quick estimate on how much fraction of monomer is effectively consumed for the growth of seeds. For this purpose, the authors will propose a simple diagram shown in Figure 6 in which only the diameters of composite and initial seed particles are to be known.

Though we observed in the preceding section that the resulting composite particles are not always spherical, and by no means reveal the so-called core–shell structure, fundamental equations may be derived assuming the structure sketched in Figure 6. Conditions to extend the correlation to general structure will be discussed later.

Suppose that N_s numbers of polymer particles of d_{s0} diameter undergo the seed polymerization, and the diameter increases to d_s after the polymerization. Introduce a parameter C defined as the fraction of monomer spent for the growth of seed polymer particles. Then one can derive the following equations:

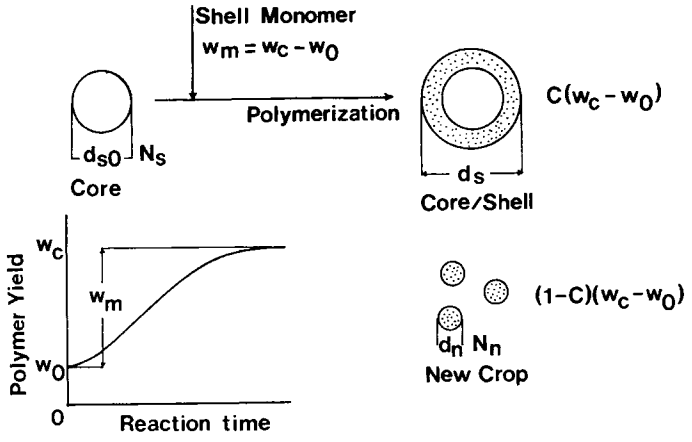

Fig. 6. Schematic diagram to derive the fraction of monomer spent for the growth of seed polymer particles, C.

$$
\begin{aligned}
C &= (w_c - w_0)(\pi/6)N_s\rho_n(d_s^3 - d_{s0}^3) \\
&= (w_c - w_0)(\pi/6)N_s\rho_s d_{s0}^3(\rho_n/\rho_s)[(d_s/d_{s0})^3 - 1] \\
&= \frac{w_0}{w_c - w_0}\frac{\rho_n}{\rho_s}\left[\left(\frac{d_s}{d_{s0}}\right)^3 - 1\right] \qquad (1) \\
&= \frac{\rho_n/\rho_s}{M/P}\left[\left(\frac{d_s}{d_{s0}}\right)^3 - 1\right]
\end{aligned}
$$

where w_0 and w_c denote initial and final polymer yield, respectively, ρ_n and ρ_s, density of shell polymer and seed (core) polymer, respectively.

Even though the resulting particles are structured as shown in Figure 5(b), Eq. (1) still holds if an assumption of the additivity of volume[7] is granted as well as the retainment of spherical shape. Proof will be straightforward.

Relationship between C and d_s/d_{s0} can be readily shown in Figure 7 with $(M/P)(\rho_s/\rho_n)$ as a parameter. Normally ρ_s/ρ_n can be regarded as unity except our cases where PVC polymers are involved.

All the experimental data taken by the authors were plotted in Figure 7 together with the results obtained by Vanderhoff et al.[8,9] with the combination of PS core and acrylonitrile AN-ST 20 : 80 comonomer.

Meanwhile it will be quite understandable that the combination of small M/P and large seed particles may give a considerable error for this plot because increase in the diameter of seed particles is barely noticeable. For example, we did not observe the nucleation of secondary particles in the experiments shown in Figure 7 with a dot mark on the shoulder; however, values of C calculated from Eq. (1) using observed d_s were extraordinarily low. At low M/P recipe, an inevitable shrinking of dry polymer particles when SEM sample is prepared will create a considerable error for this correlation. Though it may contradict the first intention of the authors, a careful detection of the secondary particles, or more accurate measurement of d_s such as the light scattering, will be recommended other than SEM.

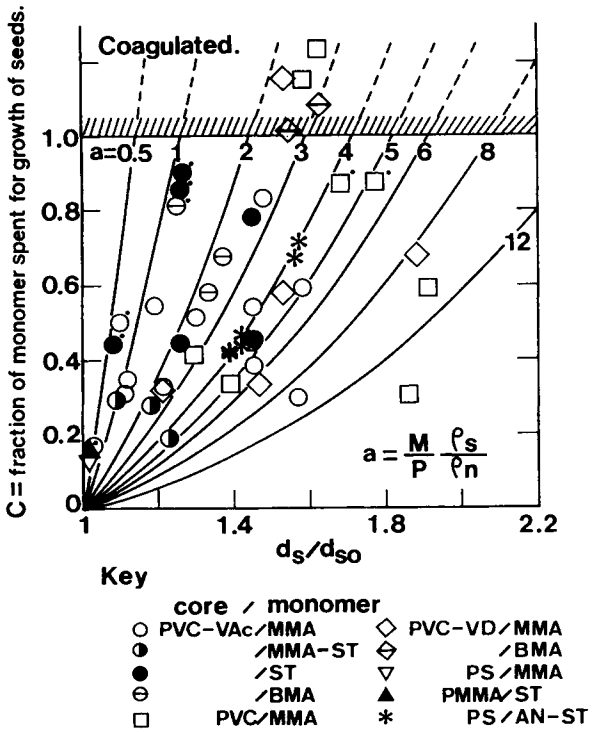

Fig. 7. Correlation between C and d_s/d_{s0}. Solid lines are calculated from Eq. (1). Data points with a dot mark on the shoulder indicates that no secondary particles are observed in SEM photographs.

When the seed particles overgrow because of the coagulation during polymerization, the plot will fall in the region of coagulation ($C > 1.0$) and certainly draw one's attention. This may another advantage of the correlation.

In Figure 7, notice that C becomes higher even though at higher M/P when smaller core particles such as PVC and PVC–VD were employed. According to Vanderhoff et al. the nucleation of secondary particles can be more easily suppressed if the surface area of seed particles per weight of shell monomer is selected higher than the certain critical values corresponding to a seed polymer–shell monomer system. In other words, the surface area, $6w_0/d_{s0}\rho_s$, increases with smaller d_{s0} provided the comparison is done based on the fixed value of initial solid content, w_0.

The surface area, defined as the unit weight of shell monomer, can be expressed as a function of M/P.

$$\frac{A}{M} = \frac{6}{d_{s0}\rho_s(M/P)} \tag{2}$$

Vanderhoff et al. claimed that the critical surface area observed in their seed polymerization system is 226 m^2/dL, which is equivalent to 9.87 m^2/g monomer calculated from Eq. (2) according to their recipe. The critical surface areas of our various seed–shell monomer systems, though in some cases determined

from only a few data, were also calculated and plotted in Fig. 8 with the calculated curves from Eq. (2).

Except for the PVC–VAc/MMA, PVC–VD/MMA and BMA systems, the critical values were fairly close to the one given by Vanderhoff et al. In principle, MMA has a tendency to nucleate the secondary particles due to the fair solubility in water. The calculated values obtained, employing smaller emulsion PMMA seeds,[10] were also plotted in Figure 8 to show the susceptibility of MMA to nucleate new particles. Even though the size of seed particles are small, the critical surface area is still high. One may speculate that the incorporation of highly polar carbonyl groups in PVC–VAc and PMMA seeds is a probable reason for the different behaviors between these seeds and PVC and PVC–VD. The size of seed polymer particles seems to be less sensitive to the critical surface area.

In the case of Vanderhoff et al., the presence of highly soluble acrylonitrile seems to become obscured due to the mixing with the sparsely soluble styrene, in favor of the latter, 20 : 80.

Consequently 11 m^2/g monomer is a good estimate to prevent the nucleation of secondary particles. It is interesting to collect more data for the plot in Figure 8 in order to confirm the concept of critical surface area as well as to propose an acceptable theory.

Results of DSC Measurement

Portion of composite particles separated from the secondary particles by means of the centrifugal procedure was used for the DSC measurement to observe thermal behavior of the samples. Transition temperatures and an exothermic peak observed at over 200°C were correlated.

Transition temperatures detected as a discontinuity of the slope were plotted against the shell fraction. Cw_m/w_c, in Figure 9(a). As already mentioned, shell

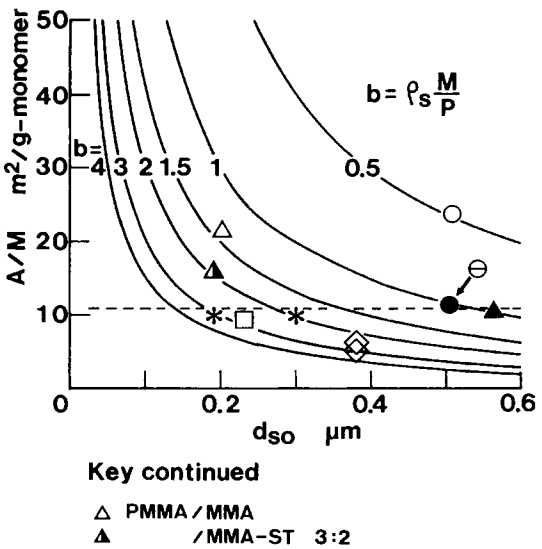

Fig. 8. Correlation between critical A/M and d_{s0}. Solid lines are calculated from Eq. (2).

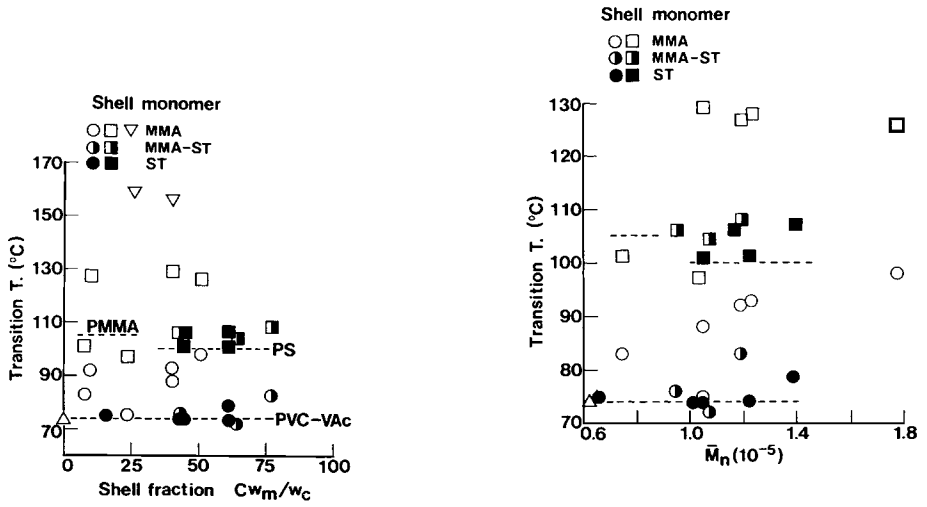

Fig. 9. Correlation of transition temperatures of composite polymer with (a) shell fraction, Cw_m/w_c, and (b) number average molecular weight, M_n.

fraction is by no means an appropriate terminology, in particular for PVA–VAc/PMMA, but may be defined as the weight fraction of shell polymer to the total polymer consisting of composite particles. The same data were then plotted against the number average molecular weight of the total polymer consisting of composite particles, M_n, as shown in Figure 9(b). Normally two transition temperatures were observed, and the third and higher one were observed with two samples of PVC–VAc/PMMA, as shown in Figure 9(a) with the ▽ symbol. The broken lines in the figure indicate reported values of the glass transition temperature, T_g, of PMMA and PS. The T_g of PVC–VAc was measured by the authors.

When either ST or MMA–ST was employed, the lower transition temperature remained on the line indicating the T_g of PVC–VAc, while the higher one being very close to that of PS or PMMA. On the other hand, in the case of MMA, the lower transition temperature gradually increased with the increase of shell fraction, while the higher one rose to as high as 130°C.

Because PMMA and PVC–VAc are miscible, a gradual increase of the lower transition temperature while increasing the shell fraction seems to support the sketch shown in Figure 5(b) that a part of PMMA becomes intermiscible with the PVC–VAc core, i.e., the lower transition temperature is a T_g of the miscible portion. On the other hand, the higher transition temperature indicates the T_g of PMMA or that raised due to the probable formation of graft linkage with PVC–VAc chains. The grafting between PS core and PAN–ST shell was substantially confirmed by Vanderhoff et al.

Two T_gs observed at around 160°C with MMA were not observed regularly. Kraus and Roman,[11] in their dilatometric measurement of the mixture of isotactic and syndiotactic PMMA, observed three transition temperatures with higher syndiotactic content (> 50%), the highest one being around 140–160°C. They claimed the T_g of 100% syndiotactic PMMA is 120°C, with no clear explanations given for the third transition temperature. The lower T_g observed

with MMA was more closely correlated with M_n of the polymer, as shown in Figure 9(b), increasing almost linearly with M_n.

The exothermic peak due to the demixing of shell and core polymers was observed just before the decomposition of polymers, and the peak temperature was correlated with the shell fraction in Figure 10(a) and with the number average molecular weight of the total polymer in Figure 10(b). No discussions were found in the previous articles concerning this peak.

The T_m in the coordinate indicates the peak temperature where demixing takes place and seems to depend on the shell fraction rather than the thermal property of each monomer, as shown in Figure 10(a). However, T_m was clearly separated in two lines, as shown in Figure 10(b) when correlated with M_n of the total polymer, the higher one with ST and MMA–ST shell and the lower with MMA shell. Another feature that may attract one's attention is that the latter line was apparently extraporated to the T_m of core polymer, PVC–VAc, at lower M_n, whereas the other lines never met.

From these figures, one may speculate that the miscibility between the shell (PS or PMMA–ST) and the core polymer is so poor that the core–shell boundary is substantially retained until the shell structure collapses. In other words, T_m is controlled by the thermal stability of the shell polymer.

On the other hand, the combination of PMMA and PVC–VAc core is regarded as fairly miscible and behaves as an ideal mixing system.

Result of TLC Measurement

From the observations with TEM and DSC, intermiscibility and a probable formation of graft linkage between PMMA and PVC–VAc core were to a great extent anticipated. In order to obtain substantial evidence, development of the polymers was done by means of TLC.

Various choices of solvent system were investigated with the particular procedure as described in the previous section. Polymer sample solution to spot is 0.25 wt % dissolved in THF. The solvent for development is a mixture of methyl

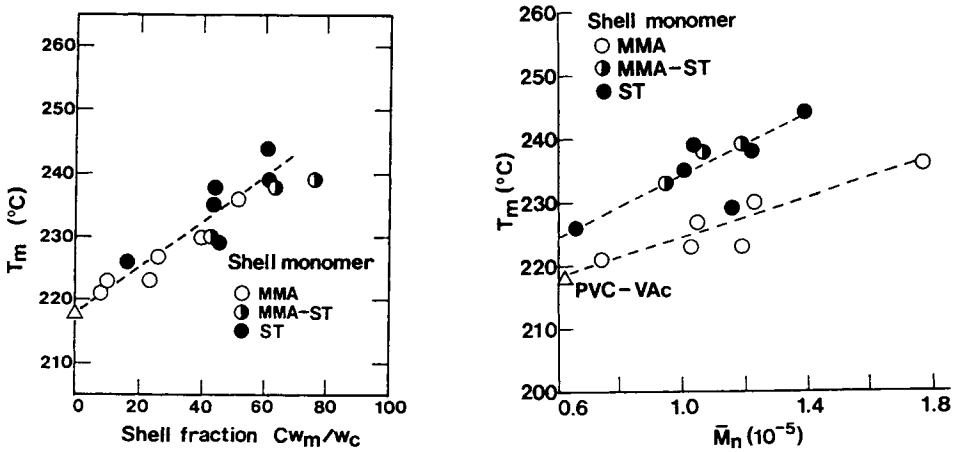

Fig. 10. Correlation of demixing temperature, T_m, of composite polymer with (a) shell fraction, Cw_m/w_c, and (b) number average molecular weight, M_n.

alcohol (MeOH) and methyl isobutylketone (MIBK), in preference to *n*-hexane and MIBK. A portion of MeOH, generally regarded as a poor solvent, was changed from 2 to 10 vol %.

The results of development for PVC–VAc copolymer, PMMA, and PS are shown in Figure 11(a). PVC–VAc is least affected by the addition of MeOH, while PS is dramatically hindered. Well-developed spectra were obtained for the PVC–VAc and PMMA samples. Though Vanderhoff et al. estimated the fraction of grafting PAN–ST from the TLC spectrum, discussion here is limited to a qualitative basis due to the inconsistent reproducibility of the spectrum.

Spectra of core–shell polymers with different shell polymer are shown in Figure 11(b). No distinguishable change was observed in the spectra of CS#17 (PMMA–ST shell) and CS#29 (PS shell) compared with the overlapped spectra of PVC–VAc and each homopolymer shown in Fig. 11(a). However, in the spectrum of CS#27 (PMMA) a less developed shoulder became clearly distinguishable, and the decrease in the shoulder peak was compensated with an increase of undeveloped fraction at the spot as the portion of MeOH increases, substantial evidence of the formation of graft PMMA–PVC–VAc. Apparently more consistent results will be obtained from the samples having smaller molecular weight. The authors intend to do a further analysis according to this speculation.

CONCLUSION

Fundamental structural features of the particular composite latices, PVC-based core probably interpenetrated with PMMA, were investigated.

A new correlation diagram—fraction of monomer spent for the growth of seeds, C vs. d_s/d_{s0}—was proposed. This correlation is quite useful for a quick evaluation with only the measurement of the particle diameter being required.

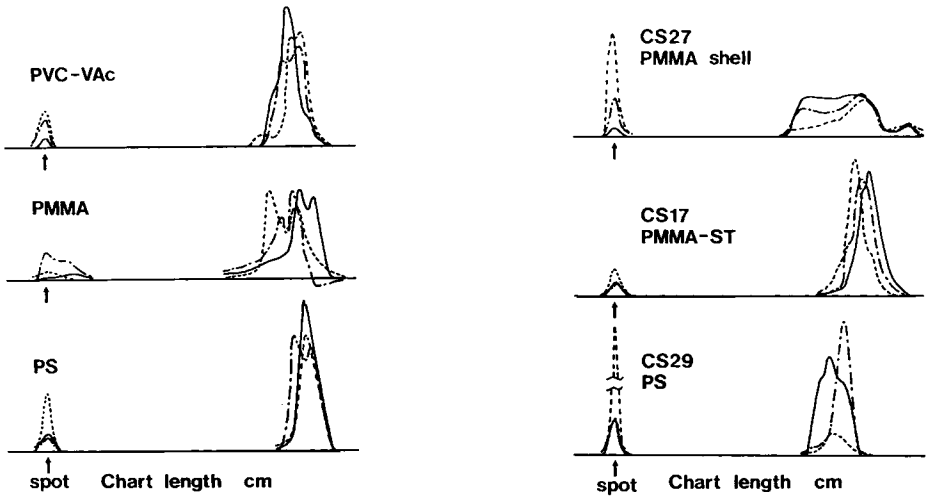

Fig. 11. TLC spectrum of related polymers. (a) PVC–VAc core, and PMMA and PS; (b) core–shell polymer with various shell polymers. Composition of the developing solvent (MeOH/MIBK): — = 2/98, -·- 5/95, and ---- = 10/90 (v/v).

Smaller M/P ratio, smaller size of seeds, and the choice of less water-soluble monomer are key factors in performing complete seed polymerization without the nucleation of secondary particles.

Vanderhoff's criterion that there exists the critical surface area of seed particles to suppress the secondary nucleation is confirmed with several combinations of seed particles and shell monomer, the critical values being found approximately 11 m^2/g monomer with a couple of exceptions. Fairly water-soluble MMA is more unpredictable and seems to depend also on the nature of seed polymer.

Neither graft linkage nor intermiscibility between the core and shell was observed when ST and MMA–ST were chosen as the shell monomer, while substantial evidence was found between PVC–VAc core and PMMA.

The authors wish to express their hearty appreciation to Dr. Shiro Ohkita, Mr. Noriaki Kuramitsu, and Ms. Hiromi Ohtsuka with Polymer Research Laboratory, Mitsui Toatsu Chemicals Inc., for providing the facility of TEM and conducting laborious works for this article.

References

1. D. J. Hoffman and P. M. Saffron, *ACS Symposium Series 165,* 209 (1981).
2. S. Oikawa, Japan Patent (Kokai Tokkyo Koho) 185518, 207418 (1986).
3. D. Gershberg, *AIChE-I. Chem. E. Symp. Ser. (London: Inst. Chem. Engrs.)* No. 3, 4 (1965).
4. J. W. Vanderhoff, *Future Directions of Polymer Colloids,* M. S. El-AAsser and R. M. Fitch, Eds., NATO ASI Series E, Appl. Sci. No. 138, 1988, p. 23.
5. O. Olabishi, L. M. Robeson, and M. T. Shaw, *Polymer-Polymer Miscibility,* Academic Press, New York, 1979, p. 217.
6. S. Akiyama, T. Inoue, and T. Nishi, *Polymer Blend—Miscibility and Interface,* CMC Co. Ltd., in Japanese, 1981, p. 69.
7. L. W. Morgan, *J. Appl. Polym. Sci.,* **27,** 2033 (1982).
8. J. W. Vanderhoff, V. Dimonie, M. S. El-Aasser, and A. Klein, *Makromol. Chem. Suppl.,* **10/11,** 391 (1985).
9. V. Dimonie, M. S. El-Aasser, A. Klein, and J. W. Vanderhoff, *J. Polym. Sci. Polym. Chem. Ed.,* **22,** 2197 (1984).
10. Y. Kuribayashi, BS thesis, Dept. Chem. Eng., Tokyo Univ. of Agri. & Tech., 1987.
11. S. Krause and N. Roman, *J. Polym. Sci. Pt. A,* **3,** 1631 (1965).

Received September 6, 1989
Accepted September 26, 1989